Preclinical verification of the efficacy by targeting peptide-linked liposomal nanoparticles for hepatocellular carcinoma therapy

Cheng-Der Wu[1], Jen-Chieh Lee[1], Hang-Chung Wu[2], Chung-Wei Lee[3], Chih-Feng Lin[4], Ming-Chen Hsu[1], and Chin-Tarng Lin[1]

Abstract

The purpose of this study was to investigate the efficacy of targeting peptides chemotherapy to overcome adverse event in the conventional chemotherapy for human hepatocellular carcinoma. Previously we reported several cancer-targeting peptides that bind specifically to cancer cells and their vascular endothelia: L-peptide (anti-cancer cell membrane), RLLDTNRPLLPY; SP-94-peptide (anti-hepatoma cell membrane), SFSHHTPILP; PC5-52-peptide (anti-tumor endothelia), SVSVGMKPSPRP; and control peptide, RLLDTNRGGGGG. In this study, these peptides were linked to liposomal iron oxide nanoparticles to localize the targeted tumor cells and endothelia, and to dextran-coated liposomal doxorubicin (L-D) to treat nonobese diabetic severe combined immunodeficient mice bearing hepatoma xenografts. Our results showed that L-peptide-linked liposomal doxorubicin could inhibit tumor growth with very mild adverse events. Use of the control peptide led to a decrease in the xenograft size but also led to marked apoptotic change in the visceral organ. In conclusion, L-peptide-linked liposomal doxorubicin, SP-94-peptide, and PC5-52-peptide can be used for the treatment of hepatoma xenografts in nonobese diabetic severe combined immunodeficient mice with minimal adverse events.

Keywords

Hepatocellular carcinoma, L-peptide, SP-94-peptide, PC5-52-peptide, peptide-targeted chemotherapy

Introduction

Hepatocellular carcinoma (HCC) is the second most frequent cause of cancer death in men and the sixth most commonly diagnosed cancer in women worldwide.[1] The prevalence of HCC varies globally. Areas of the highest rates of HCC include Southeast Asia, China, Taiwan, and sub-Saharan Africa. Eighty percent of the patients with HCC are in the Asian countries. The incidence of HCC accounts for 4% of all newly diagnosed cancers worldwide. The median survival rates are 21% and 6% at the end of 1 and 3 years, respectively. Among primary liver cancers, HCC represents the major histological subtype, accounting for 70–85% of cases of primary liver cancer.[1] Intrahepatic

[1] Institute and Department of Pathology, National Taiwan University Hospital, Taipei, Republic of China
[2] Institute of Cellular and Organismic Biology, Academia Sinica, Taipei, Republic of China
[3] Department of Medical Imaging and Radiology, National Taiwan University Hospital, Taipei, Republic of China
[4] Department of Otolaryngology, National Taiwan University Hospital, Taipei, Republic of China

Corresponding author:
Chin-Tarng Lin, Institute and Department of Pathology, National Taiwan University Hospital, No. 7 Chung-Shan South Road, Taipei 10002, Republic of China.
Email: ctl@ntu.edu.tw

cholangiocarcinoma (ICC) is the second most frequent type of liver cancer, and its incidence has also been increasing.[1,2] Both HCC and ICC are heterogeneous diseases in terms of pathological morphology and clinical outcome. Recent immunohistochemical studies of stem cell markers suggest that HCC, ICC, and HCC-ICC are histological heterogeneous and a subset of cells express a variety of stem cell markers.[3–6] The HCC markers include epithelial cell adhesion molecule, CD133, CD90, CD44, CD24, CD13, oval cell marker OV6, as well as aldehyde dehydrogenase activities. Those markers indicate that liver cancer contains highly invasive features and chemoresistance.[6–12]

Liver cancer frequently develops in chronic liver disease, in which continuous inflammation and hepatocyte regeneration occur.[13] Chronic viral hepatitis, particularly when caused by the hepatitis B virus, is the most important risk factor for the development of HCC in Taiwan.[14] In addition to some genetic alterations, pathophysiological changes occur during the processes of inflammation and regeneration to promote liver cell transformation. These processes include the expansion of transformed (stem/progenitor) cells, with the accumulation of genetic and/or epigenetic changes, and alteration of the microenvironment.[14–18] Currently, the "cancer initiating/ or stem cell" theory may partially explain the process of HCC formation. According to the theory, there is a small population of stem-like cells in tumor tissue, known as liver cancer stem cells, which are responsible for self-renewal, direct invasion, metastasis, and chemoresistance. Deregulation of signaling pathways, including the transforming growth factor β, Wnt, Notch and Hedgehog pathways have been found to be involved in the process of hepatocarcinogenesis.[19–39]

Over the past decade, liver cancer survival has been steadily improving as a result of developments in surgery, transplantation, and chemotherapy. The introduction of a number of novel, local, ablative, and molecular-targeted therapies[32] also has the potential to downstage patients so they are eligible for curative treatment.[39] However, the survival rate for the advanced late stage patients remains less optimistic. The efficacy of systemic cytotoxic chemotherapy has previously been widely assessed in patient with advanced HCC; for example, doxorubicin, whether in combination with other agents or as a single treatment, is the most commonly studied chemotherapeutic agent for HCC. Doxorubicin has been shown to have a response rate of 10–20% in clinical trial,[33] but its potential benefit is hindered by treatment-related adverse effects.[33] Radiotherapy and transarterial chemoembolization can also be used for complement chemotherapy in the treatment of unrespectable HCC.[40] So far, the multikinase inhibitor sorafenib[40] is thought to provide survival benefits over supportive care. However, the long-term prognosis of those HCC patients still remains poor.

Previously, we had identified the target of the peptide was GRP78 protein.[41] We reported that the normal liver cells cannot be bound by the peptide. Therefore, in the present experiment, we proposed to use the peptide-targeted chemotherapy to overcome the adverse effect in the conventional chemotherapy. The peptides that we used included the L-peptide (L-P),[42] PC5-52-peptide (PC5-52-P),[43] and SP-94-peptide (SP-94-P).[44] The L-P was derived from a phage-displayed 12-mer random peptide library used to screen binding activity in a nasopharyngeal carcinoma (NPC) cell line (NPC-TW01 cell line).[42] Although L-P was initially shown to bind specifically the NPC tumor cells but not normal cells both in vitro and in vivo, it was later demonstrated to be a multifunctional peptide that binds to different cancer cell lines, including hepatoma cell lines.[45] Using a similar phage-displayed 12-mer random peptide library to screen HepG2 liver cancer and the pulmonary adenocarcinoma (CL1-5) xenograft,[43] we have also identified another two peptides, such as SP-94-P[44] and PC5-52-P,[43] which can specifically bind to hepatoma cell (HepG2 and Huh-7) and pancreatic cancer cell (panc-1),[43] and to lung cancer endothelial cells,[42] respectively. The use of these peptides in peptide-targeted chemotherapy for hepatoma is described in the present study.

Materials and methods

Peptides, cell lines, surgical specimens, and animals

We linked the following peptides to liposomal iron oxide (L-Fe_3O_4) nanoparticle and liposomal doxorubicin (L-D): L-P, RLLDTNRPLLPY,[42] obtained from NPC; control peptide (C-P), RLLDTNRGGGGG, and SP-94-P, SFSIIHTPILPL,[43] obtained from hepatoma; and PC5-52-P, SVSVGMKPSPRP,[43] obtained from lung cancer endothelia. The L-P, SP-94-P, and PC5-52-P were obtained from Genomics BioSci Tech. Co., Ltd (Taipei, Taiwan); the dextran-coated iron oxide (Fe_3O_4) was purchased from a commercial source (MagQu Co., Ltd, Taipei, Taiwan).

Liposomes composed of distearoylphosphatidylcholine, cholesterol, and PEG-DSPE were hydrated at 55°C in an ammonium sulfate solution (250 mmol/L $(NH4)_2SO_4$ (pH 5.0) and 530 mOsm) and extruded through polycarbonate membrane filters (Costar, Cambridge, Massachusetts, USA) of 0.1 and 0.05 μm pore size with high-pressure extrusion equipment (Lipex Biomembranes, Vancouver, British Columbia, Canada) at 60°C, and doxorubicin was encapsulated in the liposomes by a remote loading method at a concentration of 1 mg of doxorubicin per 10 μmol phospholipid. The final concentration of liposomes was determined by phosphate assay. After adding 1 mL of acidic isopropanol (81 mmol/L HCl) to 0.2 mL of diluted drug-loaded liposomes, the amount of doxorubicin trapped inside the liposomes was determined with a spectrofluorometer (Hitachi F-4500; Hitachi, Ltd, Tokyo, Japan) with 470 nm as excitation wavelength and 582 nm as emission wavelength. Vesicle sizes were measured by dynamic laser scattering with a submicron particle analyzer (model N4 plus; Coulter Electronics, Hialeah, Florida, USA). After preparation, the liposomes contained 110–130 μg doxorubicin per μmol phospholipid and had a particle size ranging
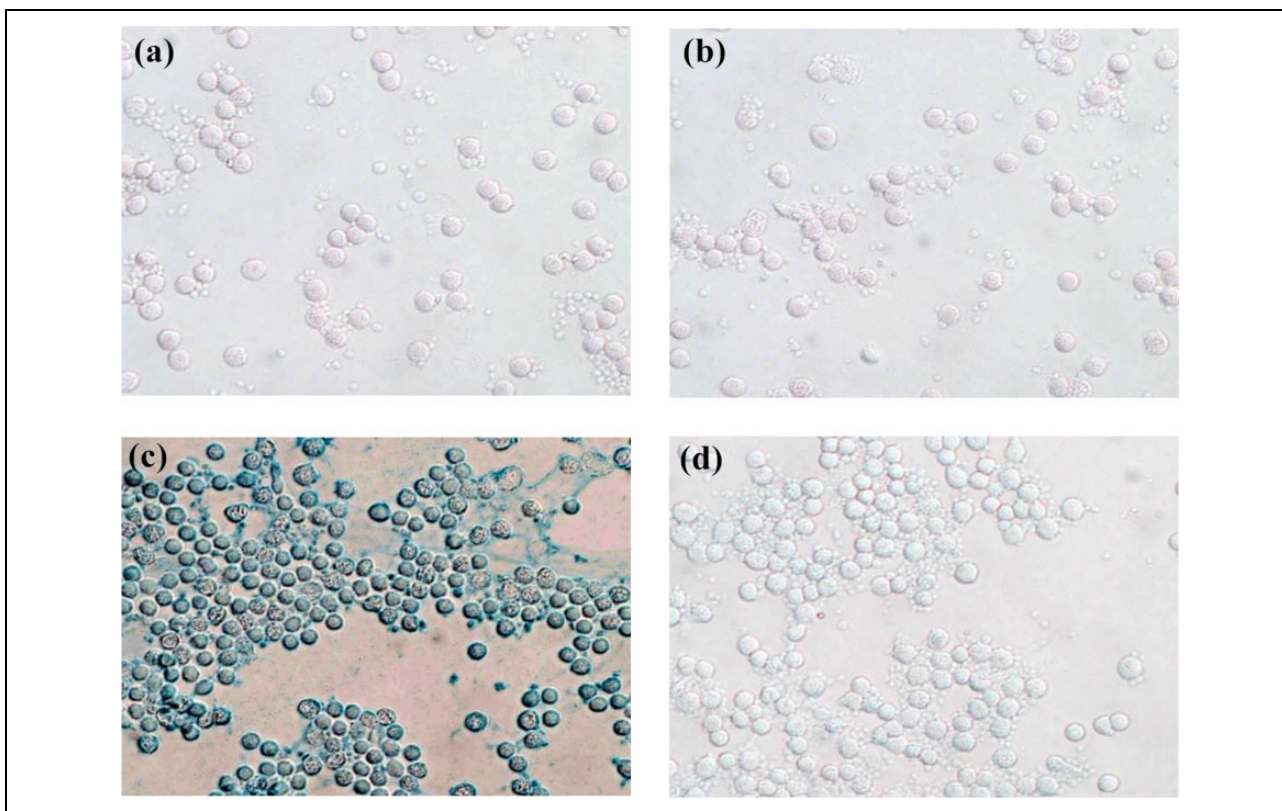
Figure 1. Peptide histochemical localization of L-P-targeted protein in peripheral blood cells. No reaction product was observed after Prussian blue staining of untreated blood smears which were incubated with either L-P-Fe3O4 (a) or C-P-Fe3O4 (b). However, iron oxide reaction product was observed in the cytoplasm of mononuclear cells of blood smears after they were treated with Triton X-100 and incubated with L-P-Fe3O4 (c), whereas no positive staining was seen in the smears which were incubated with C-P-Fe3O4 (d). To verify whether L-P-L-Fe3O4 could bind specifically to the targeted cancer cell membrane protein but not the normal cell membrane, we isolated the peripheral blood mononuclear cells and treated with L-P-L-Fe3O4. L-P: L-peptide; C-P: control peptide; Fe3O4: iron oxide; L-Fe3O4: liposomal iron oxide.

from 65 to 75 nm in diameter. For encapsulation of the fluorescent substance HPTS (trisodium salt), small unilamellar vesicles were prepared by reverse-phase evaporation. At a molar ratio of 2:1, EPC (egg phosphatidylcholine) and cholesterol were extruded repeatedly through polycarbonate membrane filters of pore sizes of 0.1 and 0.05 μm sequentially. A solution of liposomes encapsulating 30 mmol/L HPTS was prepared in distilled water. The same method was used to prepare a C-P to replace the L-P and couple to NHS-PEG-DSPE for comparison. Peptidyl-PEG-DSPE was transferred to preformed liposomes after co-incubation at temperature above the transition temperature of lipid bilayer. Three hundred to five hundred peptide molecules per liposome were formed.

Two HCC cell lines, HepG2, and Huh-7, were obtained from the American Type Culture Collection. Both cell lines were cultured in the Dulbecco's modified Eagle medium containing 5% fetal calf serum and incubated in the 10% CO_2 incubator as the routine cell culture conditions. Thirty HCC surgical specimens were obtained from the archives of the Department of Pathology at the National Taiwan University Hospital (NTUH; Taipei, Taiwan), with the

approval for usage by the NTUH Institutional Review Board (#201103029RC). Nonobese diabetic severe combined immunodeficient (NOD SCID) mice and NOD SCID gamma (NSG) mice were obtained from and investigated at the NTUH animal center. The use of animals was approved and regulated by the Institutional Animal Care and Use Committee in the College of Medicine (#20150162).

Localization of the peptide-targeted protein in hepatocellular carcinoma cell lines and their surgical specimens

Individual L-P, SP-94-P, and PC5-52-P bind weakly to the targeted proteins in the cancer cell lines and surgical specimens; using peptide-linked dextran-coated iron oxide (P-Fe_3O_4) nanoparticles with a conventional Prussian blue reaction to localize their targeted proteins. Briefly, we prepared L-P-linked dextran-coated iron oxide nanoparticles such as L-P-Fe_3O_4, SP-94-P-Fe_3O_4, PC5-52-P-Fe_3O_4, and C-P-Fe_3O_4 nanoparticles. The dextran-coated iron oxide nanoparticles were purchased from MagQu Company.[20,21] Then the L-P, SP-94-P, and PC5-52-P were conjugated to
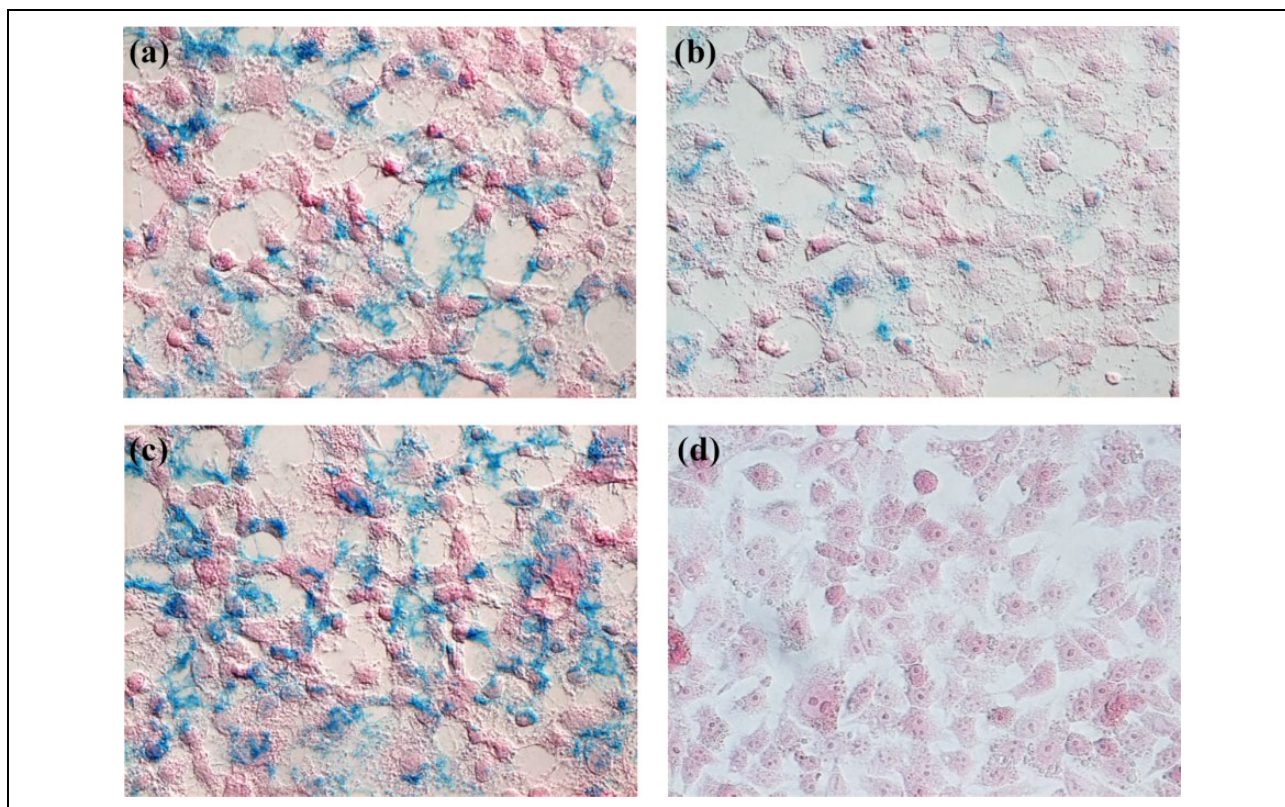
Figure 2. Peptide histochemical localization of L-P-targeted protein in hepatoma cancer cell line. Triton X-100-treated HepG2 cells after incubated with L-P-Fe3O4 showed positive Prussian blue staining, while a little bit lower stained cells were observed in the cell culture incubated with SP-94-P-Fe3O4. However, when HepG2 cells were incubated with the L-P-Fe3O4 + SP-94-P-Fe3O4 mixture, an increase in the number of stained tumor cells was observed. (a) L-P-Fe3O4, (b) SP-94-P-Fe3O4, (c) L-P + SP-94-P-Fe3O4 (1:1), and (d) C-P-Fe3O4. L-P: L-peptide; C-P: control peptide; Fe3O4: iron oxide.

dextran-coated iron oxide. Each dextran-coated iron oxide can be linked to more than 10 peptide molecules.[22,23] To localize the peptide-targeted protein in the HepG2 and Huh-7 cell lines, we first have to determine whether our peptide was able to bind to mononuclear cells in the human peripheral blood. The mononuclear cells were obtained from the normal human blood using Histopaque-1077 cell separation medium (Sigma, St. Louis, Missouri, USA). Blood smears were fixed by formaldehyde, treated with or without Triton X-100, stained with 40 µg per mL of L-P-Fe$_3$O$_4$, SP-94-P-Fe$_3$O$_4$, or C-P-Fe$_3$O$_4$, separately, and then subjected to the Prussian blue reaction with nuclear fast red staining. The same staining protocol, with the addition of a 1:1 of L-P-Fe$_3$O$_4$:SP-94-P-Fe$_3$O$_4$ staining mixture, was used to stain the HepG2 and Huh-7 tumor cells. Paraffin-embedded sections of HCC surgical specimens underwent deparaffinization and antigen retrieval of targeted protein molecule as part of the routine immunohistochemistry[34] and were incubated overnight with 40 µg per mL of L-P-Fe$_3$O$_4$, SP-94-P-Fe$_3$O$_4$, or a mixture of L-P-Fe$_3$O$_4$ and SP-94-P-Fe$_3$O$_4$ at 1:1 ratio. Sections were then stained with Prussian blue and counterstained for 2 min with nuclear fast red solution. This method was used to examine 30 HCC surgical specimens. The Prussian blue-stained cell numbers in each paraffin section were counted in 10 high power fields (400×).

Magnetic resonance imaging analyses of HepG2 and Huh-7 xenografts in animal experiment

A clinical 7 Tesla (T) magnetic resonance imaging (MRI) system (Signal Excite, GE, Milwaukee, Wisconsin, USA) was used. Under gas anesthesia with 2% isoflurane, each mouse was placed in a homemade resonance coil with an inner diameter of 3.7 cm. For characterization of imaging capability of nanoparticles (10 µg/mL PBS) serial dilution of these nanoparticles was performed. For comparison, a free Dex-Fe$_3$O$_4$ and L-P-Dex-Fe$_3$O$_4$ were also examined. After incubation of 10 µg/mL PBS of nanoparticles with 1×10^7 cancer cells in 0.2 mL PBS, then were placed in 0.5 mL tubes and incubation to 4°C for 1 h, and moved to 37°C for 2 h. Gradient echo pulse sequences provided by the vendor were used (TR/TE 5000/56 ms, flip angle 150, matrix size 256×256). The slice thickness was 1 mm with a 1 mm gap, and the field of view was 14×10.5 cm^2 for coronal scanning of the test tube, and a scan time of 8 min and 2 s was used for sagittal scanning at the NEX of 3. The images were subsequently analyzed at the workstation provided by GE
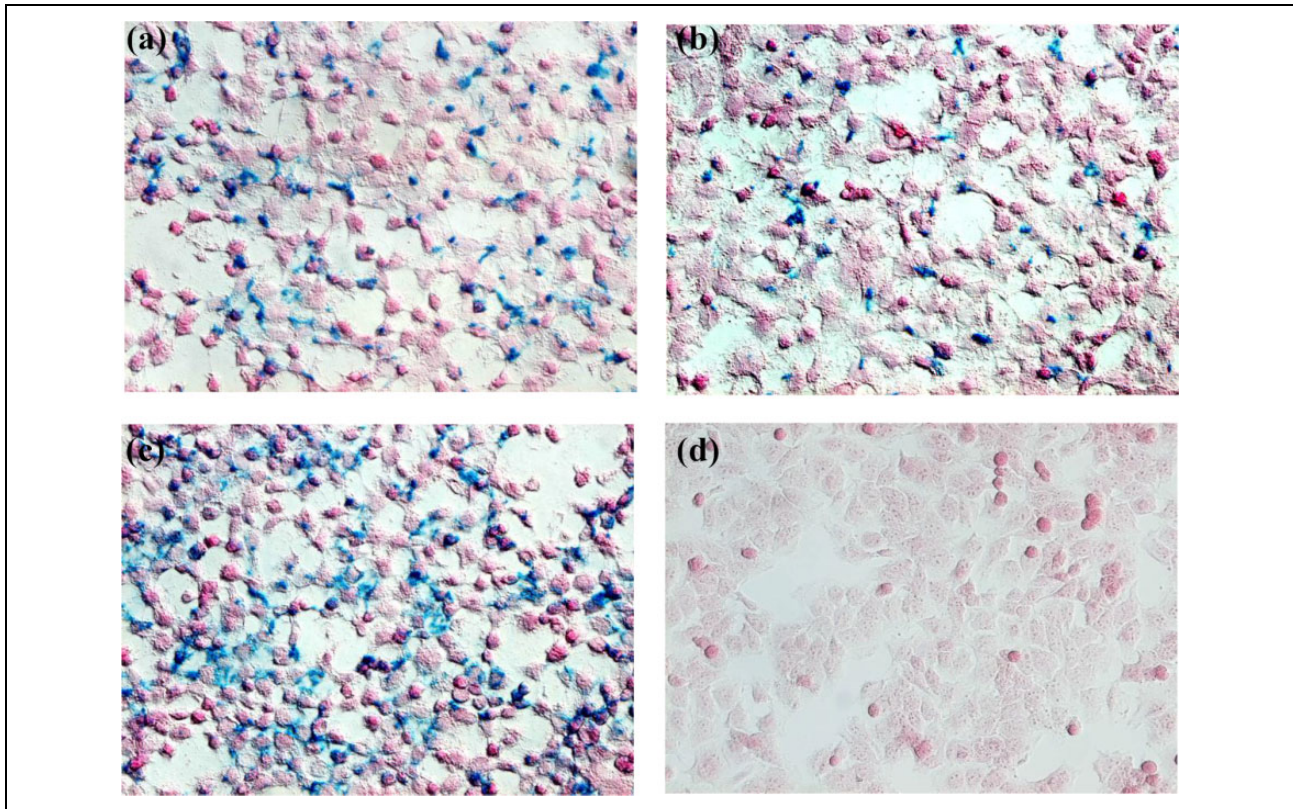
Figure 3. Peptide histochemical localization of L-P-targeted protein in hepatoma cancer cell line. When the Huh-7 cells were treated with the same protocol, a slightly larger number of stained cells after incubated with L-P-Fe3O4 was seen when compared with SP-94-P-Fe3O4 treatment; but if the cells were incubated with the combination of both peptide-linked Fe3O4, the result showed more stained cells than the individual peptide. (a) L-P-Fe3O4, (b) SP-94-P-Fe3O4, (c) L-P + SP-94-P-Fe3O4 (1:1), and (d) C-P-Fe3O4. L-P: L-peptide; C-P: control peptide; Fe3O4: iron oxide.

Healthcare. We used the MRI signal intensity before the injection as the control to show the differences after the injection in the same xenografts and mice. This approach helps avoid the bias from different tumors or mice. The signal to noise ratio dropped 54% after L-P-Fe$_3$O$_4$ was injected.

The efficacy of peptide-linked liposomal doxorubicin treatment in severe combined immunodeficient mice bearing HepG2 xenografts

To test the efficacy of peptide-targeted chemotherapy, each of 80 NOD SCID mice (40 males and 40 females) received subcutaneous injection of 1×10^7 HepG2 cells in the right thigh. After 10 days, solid xenografts measuring approximately 0.8 cm in diameter were found in each mouse. The mice were divided into two subgroups with 20 male and 20 female mice in each subgroup. Each subgroup of male and female mice was injected with 0.2 mL of either PBS or 2 mg doxorubicin per kg of mouse body weight of L-P-L-D, PC5-52-P-L-D, or L-P-L-D + PC5-52-P-L-D (1:1 mg ratio). Each mouse was injected through the tail vein for a total of four injections. The body weight and tumor size were measured weekly. All animals were euthanized

Table 1. Comparison of the staining results in hepatoma tumor cells with different peptide-linked L-Fe$_3$O$_4$ treatment ($N = 30$).[a]

	Average percentage of stained tumor cell number		
Peptide	<25%	25–50%	>75%
L-peptide-Fe$_3$O$_4$	6	7	17
P13-peptide-Fe$_3$O$_4$	6	9	15
SP94-peptide-Fe$_3$O$_4$	5	9	16

L-Fe$_3$O$_4$: liposomal iron oxide.
[a]Ten high power view ($\times$400).

1 week after the last injection and underwent routine autopsy. Histopathological sections of xenograft tumors and all visceral organs were stained with hematoxylin and eosin and examined under the routine light microscope. The pegylated L-D was a gift from the Taiwan Liposome Company in Taiwan, and pegylated peptide was linked to L-D in our laboratory using our previously published methods.[42] For comparison, the same experimental protocol was preformed using NSG mice. We injected the xenograft bearing NSG mice with 2 mg per kg body weight of L-P-L-D, SP94-P-L-D, or a mixture of L-P-L-D + SP-94-P-L-D at a 1:1 ratio once per week as mentioned above for
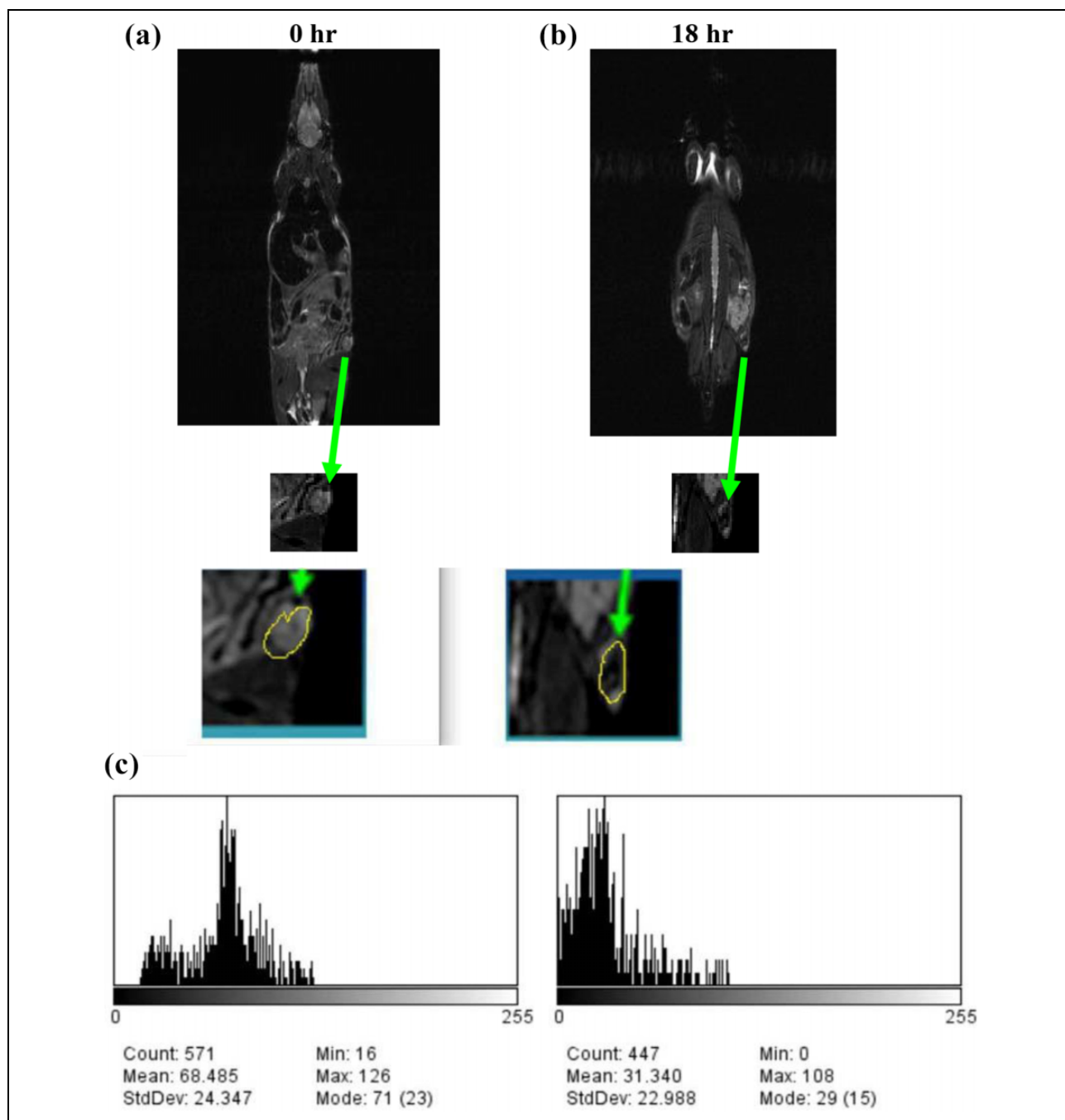
Figure 4. The MRI analysis of HepG2 xenografts in the mice either 18 h before or after injection with L-P-Fe3O4 showed that the signal intensity in the xenograft masses was lower in post-injection case ((b), arrow) when compared with the imaging before injection ((a), arrow). But injection of L-P-F3O4, led to marked decrease in MRI signal intensity when compared with the pre-injection condition (c). L-P: L-peptide; Fe3O4: iron oxide; SCID: severe combined immunodeficient; MRI: magnetic resonance imaging.

5 weeks. Thereafter, the animals were euthanized for histopathological examination too.

Statistical analysis

Contractility data are presented as the mean $\pm$ standard error. Statistical analyses were performed using Student's t-test for paired or unpaired data, as applicable. Comparisons between groups were performed using a one-way factorial analysis of variance followed by the Tukey's post hoc test. A p value less than 0.05 was accepted as significant.

Results and discussion

The results (Figure 1) indicate that L-P does not bind to the targeted protein on the normal blood cell membranes, but
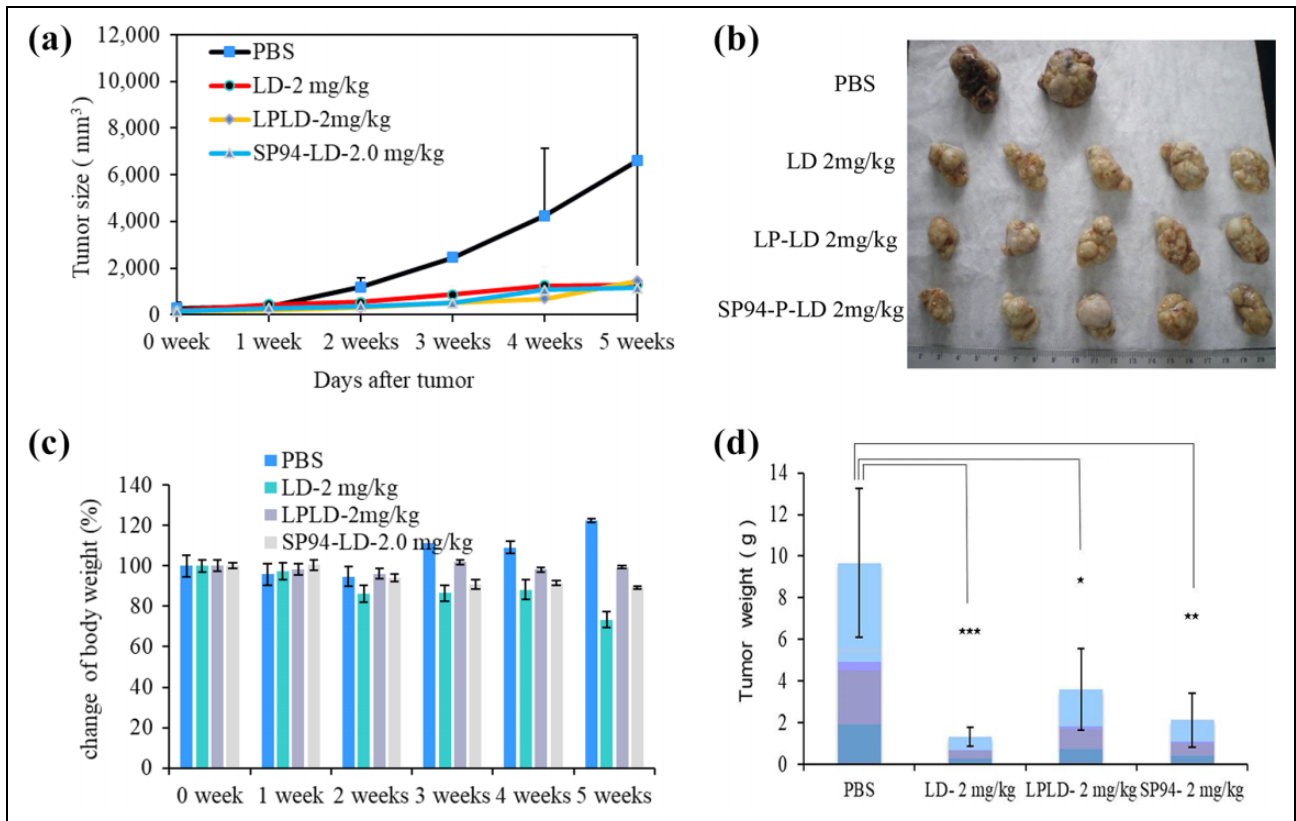
Figure 5. Treatment of NOD SCID mice bearing HepG2 xenografts using L-P-L-D (2 mg/kg, once/week/4 doses). (a) The tumor size, (b) the tumor picture, (c) the change of mice body weight, and (d) the tumor weight (*$p < 0.05$; **$p < 0.01$; ***$p < 0.001$). NOD SCID: nonobese diabetic severe combined immunodeficient; L-P: L-peptide; L-D: liposomal doxorubicin.

bind to the fixed and detergent-treated cytoplasmic target protein in normal mononuclear cells, indicating that L-P binding protein is only present in the cytoplasm of normal cells. It is clear that L-P-L-Fe_3O_4 can bind to its target protein on the membrane of hepatoma cells (Figures 2 and 3), but not the normal mononuclear cell membrane. Using the Prussian blue staining method for the localization of the L-P-targeted protein with L-P-Fe_3O_4 as described previously,[41] we showed that the Prussian blue reaction product was easily identified in the tumor cells in stained sections. Although some tumor cells that had infiltrated the surrounding liver tissue also showed the blue reaction product (Figure 1(a) to (d)), the stromal cells and some other tumor cells in the tumor nests still showed no staining (Figure 1(a) to (c)); incubation of the HCC surgical specimens with SP-94-P-Fe_3O_4 led to the same staining pattern as observed with L-P-Fe_3O_4. Approximately 70–90% of the tumor cells in each of the 30 HCC surgical sections showed positive staining (Table 1). When the sections were incubated with a combination of two kinds of peptide-Fe_3O_4, the results showed slightly higher numbers of stained cells (data not shown). However, some unstained tumor cells were still identifiable. Furthermore, L-P can also bind to the cytoplasm of many HCC cells in the tumor mass section, and to the infiltrating tumor cells surrounding normal

hepatocytes, and also to the cytoplasm of infiltrating mononuclear cells but not normal hepatocytes, Kupffer cells or normal endothelial cells.

There was no significant difference in MRI signal intensity of HepG2 xenografts in the NOD SCID mice before or after injection with L-Fe_3O_4 (Figure 4). These results indicate that L-P-L-Fe_3O_4 is also potentially useful for clinical identification of hepatoma nodule in the patient by MRI. To demonstrate the specific targeting of the peptide to cancer cells, although the cell staining with a small fluorophore-labeled peptide may be better than our Fe_3O_4 nanoparticles, but the presence of large liposomal iron oxide particles may affect the binding of the peptide[The sentence "To demonstrate the specific targeting of the peptide to cancer cells…" seems unclear. Please correct the sentence as needed.]. Furthermore, the fluorophore-labeled peptide cannot be demonstrated by MRI in vivo.

After weekly treatment for 5 weeks, the size of the xenografts in the NOD SCID mice had reduced 85% in the L-P-L-D, SP-94-P-L-D, and L-P-L-D + SP-94-P-L-D groups when compared with the PBS and L-D groups (Figure 5(a)). No significant change of body weight was shown in those five groups (Figure 5(c)), and the average xenograft weight ratio for PBS:L-D:L-P-L-D:SP-94-P-L-D was 1:3:2:2 (Figure 5(d)). However, the histopathological data
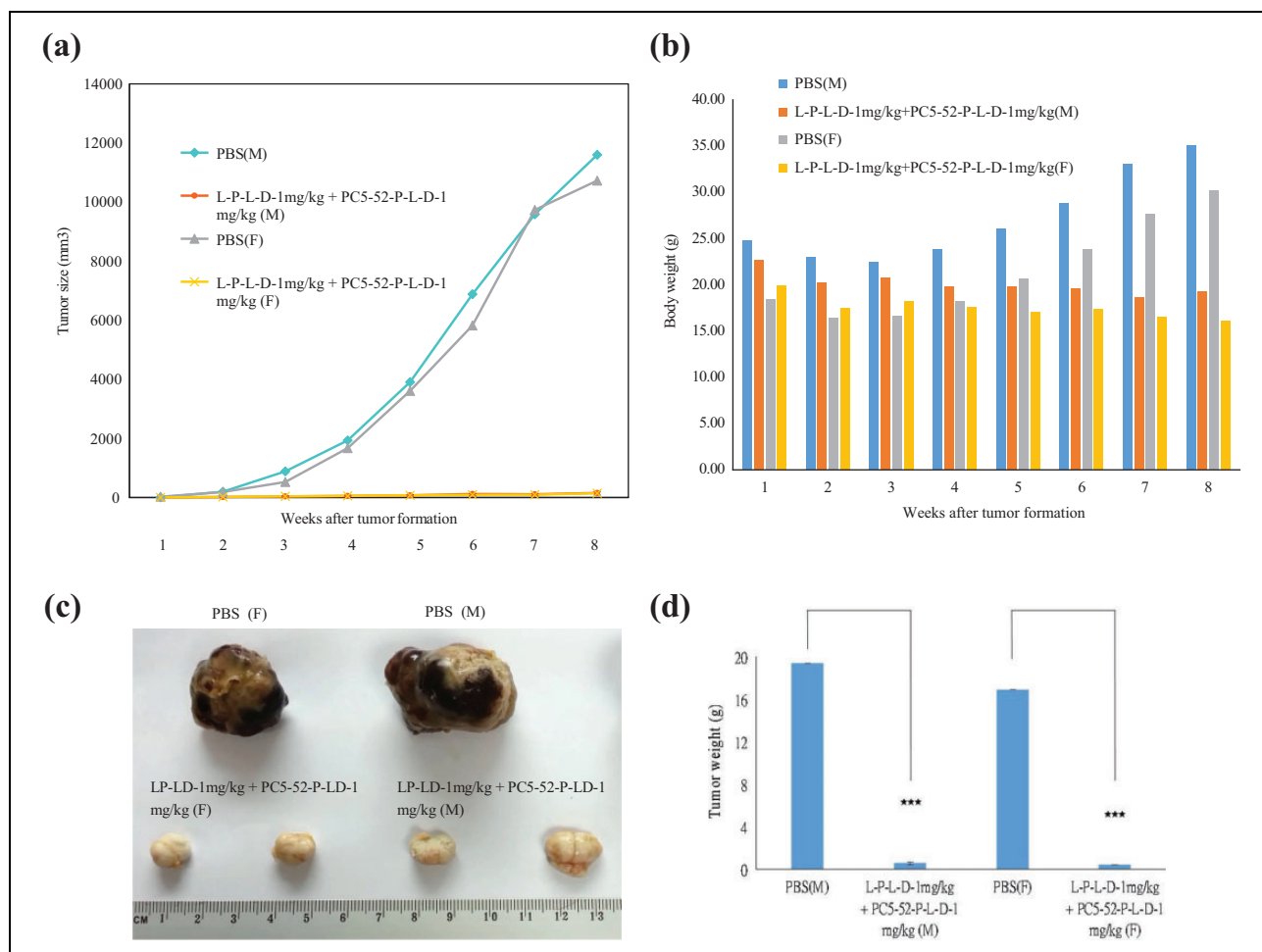
Figure 6. Treatment of NSG mice bearing HepG2 xenografts using PBS, L-P-L-D (1 mg/kg) + PC5-52-P-L-D (1 mg/kg, once/week, total 8 weeks). (a) The tumor size, (b) the tumor picture, (c) the change of mice body weight, and (d) the tumor weight (***$p < 0.001$). L-P: L-peptide; L-D: liposomal doxorubicin; NSG: nonobese diabetic severe combined immunodeficient gamma.

of the xenografts in the L-D, L-P-L-D, SP-94-P-L-D, and L-P-L-D + SP-94-P-L-D groups revealed a remarkably different feature. In the PBS control group, tumor cells showing ischemic necrosis were found in the central part of the tumor, while the peripheral zones were all normal. In the L-D-treated group, necrotic and apoptotic areas were localized in the central part of the tumor, and extended to some peripheral part of the xenograft, whereas other parts of the xenograft revealed original tumor cells with many mitotic features. The L-P-L-D-, SP-94-P-L-D-, and L-P-L-D + SP94-P-L-D-treated groups showed marked tumor necrosis and disseminated apoptosis in the whole xenograft. All L-P-L-D-, SP-94-P-L-D-, and L-P-L-D + SP-94-P-L-D-treated mice revealed no clear abnormalities in the visceral organs, which included the cardiac muscle, the liver, the kidney, the spleen, and the bone marrow. The bone marrow and cardiac muscle of L-D-treated mice showed no specific change, but the liver revealed sporadic vesicular degeneration in most hepatocytes, and apoptotic change in some hepatocytes, while the kidney also showed focal necrosis and apoptosis of some proximal tubular

epithelia. Additionally, the examination of the spleen revealed apoptotic changes in certain megakaryocytes (data not shown), which is a similar result to that shown in our previous publication.[44] It is apparent that a combination of two different peptide-linked L-D is more efficient than that of a single peptide-linked L-DW to cause hepatoma tumor cell necrosis. When we used a combination of 1mg/kg of L-P-L-D + 1mg/kg of PC5-52-P-L-D (1:1 ratio) to treat NSG mice bearing hepatoma xenografts, which produced better results than that of the combination of L-P-L-D + SP-94-P-L-D treatment in NOD SICD mice. In addition, if we injected tumor bearing NSG mice with (a) 0.5 mg per kg of L-P-L-D, once per week for 4 weeks followed by 0.5 mg/kg of PC5-52-P-L-D once per week for another 3 weeks, or (b) 1 mg per kg of L-P-L-D once per day for 4 weeks plus 1 mg/kg of PC5-52-P-L-D once per week for 3 weeks, the results of those combination of treatment revealed better result than that of the combination of different peptide-linked L-D treatment. In the evaluation of the optimal dose of L-P-L-D for a high efficacy with minimal adverse events in NOD SCID mice bearing HepG2 xenografts (Figure 6),

we found that 1 mg per kg body weight of L-P-L-D could partially inhibit tumor growth (Figure 6(a)), while 2 mg per kg of L-P-L-D could result in a marked reduction of the tumor size. In addition, the use of PC5-52-P-L-D in combination with L-P-L-D and SP-94-P-L-D could result in relatively higher chemotherapeutic efficacy for HCC (Figure 6(d)). In other words, using an anti-tumor cell peptide in combination with an anti-endothelial peptide is more effective than that of using a combination of two different anti-tumor cell peptides.

In conclusion, the better efficacy could be obtained when the anti-tumor cell peptide L-D was used in combination with the anti-endothelial peptide L-D.

Declaration of conflicting interests

The author(s) declared no potential conflicts of interest with respect to the research, authorship, and/or publication of this article.

ORCID iD

Chin-Tarng Lin https://orcid.org/0000-0003-3928-1412

References

1. Jemal A, Bray F, Center MM, et al. Global cancer statistics. *CA Cancer J Clin* 2011; 61(2): 69–90.
2. De Jong MC, Nathan H, Sotiropoulos GC, et al. Intrahepatic cholangiocarcinoma: an international multi-institutional analysis of prognostic factors and lymph node assessment. *J Clin Oncol* 2011; 29(23): 3140–3145.
3. Parkin DM, Bray F, Ferlay J, et al. Global cancer statistics, 2002. *CA Cancer J Clin* 2005; 55: 74–108.
4. Komuta M, Spee B, Vander Borght S, et al. Clinicopathological study on cholangiolocellular carcinoma suggesting hepatic progenitor cell origin. *Hepatology* 2008; 47(5): 1544–1556.
5. Ma S, Chan KW, Hu L, et al. Identification and characterization of tumorigenic liver cancer stem/progenitor cells. *Gastroenterology* 2007; 132(7): 2542–2556.
6. Yamashita T, Ji J, Budhu A, et al. EpCAM-positive hepatocellular carcinoma cells are tumor-initiating cells with stem/progenitor cell features. *Gastroenterology* 2009; 136(3): 1012–1024.
7. Haraguchi N, Ishii H, Mimori K, et al. CD13 is a therapeutic target in human liver cancer stem cells. *J Clin Invest* 2010; 120(9): 3326–3339.
8. Yang ZF, Ho DW, Ng MN, et al. Significance of CD90^{+} cancer stem cells in human liver cancer. *Cancer Cell* 2008; 13(2): 153–166.
9. Lee TK, Castilho A, Cheung VC, et al. CD24^{+} liver tumor-initiating cells drive self-renewal and tumor initiation through STAT3-mediated NANOG regulation. *Cell Stem Cell* 2011; 9(1): 50–63.
10. Ma S, Chan KW, Lee TK, et al. Aldehyde dehydrogenase discriminates the CD133 liver cancer stem cell populations. *Mol Cancer Res* 2008; 6(7): 1146–1153.
11. Yang W, Wang C, Lin Y, et al. OV6^{+} tumor-initiating cells contribute to tumor progression and invasion in human hepatocellular carcinoma. *J Hepatol* 2012; 57(3): 613–620.
12. Chiba T, Kita K, Zheng YW, et al. Side population purified from hepatocellular carcinoma cells harbors cancer stem cell-like properties. *Hepatology* 2006; 44(1): 240–251.
13. Thorgeirsson SS and Grisham JW. Molecular pathogenesis of human hepatocellular carcinoma. *Nat Genet* 2002; 31(4): 339–346.
14. Nowell PC. The clonal evolution of tumor cell populations. *Science* 1976; 194(4260): 23–28.
15. Roskams T. Liver stem cells and their implication in hepatocellular and cholangiocarcinoma. *Oncogene* 2006; 25(27): 3818–3822.
16. Oertel M and Shafritz DA. Stem cells, cell transplantation and liver repopulation. *Biochem Biophys Acta* 2008; 1782(2): 61–74.
17. Clouston AD, Powell EE, Walsh MJ, et al. Fibrosis correlates with a ductular reaction in hepatitis C: roles of impaired replication, progenitor cells and steatosis. *Hepatology* 2005; 41(4): 809–818.
18. Saxena R and Theise N. Canals of Hering: recent insights and current knowledge. *Semin Liver Dis* 2004; 24(1): 43–48.
19. Scadden DT. The stem-cell niche as an entity of action. *Nature* 2006; 441(7097): 1075–1079.
20. Feitelson MA and Lee J. Hepatitis B virus integration, fragile sites, and hepatocarcinogenesis. *Cancer Lett* 2007; 252(2): 157–170.
21. Farazi PA and DePinho RA. Hepatocellular carcinoma pathogenesis: from genes to environment. *Nat Rev Cancer* 2006; 6(9): 674–687.
22. Hussain SP, Schwank J, Staib F, et al. TP53 mutations and hepatocellular carcinoma: insights into the etiology and pathogenesis of liver cancer. *Oncogene* 2007; 26(15): 2166–2176.
23. Thompson MD and Mona SP. WNT/β-catenin signaling in liver health and disease. *Hepatology* 2007; 45(5): 1298–1305.
24. Christine G, Sagmeister S, Schrottmaier W, et al. Up-regulation of the fibroblast growth factor 8 subfamily in human hepatocellular carcinoma for cell survival and neoangiogenesis. *Hepatology* 2011; 53(3): 854–864.
25. Roskams T, De Vos R, Van Eyken P, et al. Hepatic OV-6 expression in human liver disease and rat experiments: evidence for hepatic progenitor cells in man. *J Hepatol* 1998; 29(3): 455–463.
26. Huang HP, Chen PH, Yu CY, et al. Epithelial cell adhesion molecule (EpCAM) complex proteins promote transcription factor-mediated pluripotency reprogramming. *J Biol Chem* 2011; 286(38): 33520–33532.

27. Takahashi K, Tanabe K, Ohnuki M, et al. Induction of pluripotent stem cells from adult human fibroblasts by defined factors. *Cell* 2007; 131(5): 861–872.

28. Takahashi K and Yamanaka S. Induction of pluripotent stem cells from mouse embryonic and adult fibroblast cultures by defined factors. *Cell* 2006; 126(4): 663–676.

29. Hong H, Takahashi K, Ichisaka T, et al. Suppression of induced pluripotent stem cell generation by the p53-p21 pathway. *Nature* 2009; 460(7259): 1132–1135.

30. Jochen U, Polo JM, Stadtfeld M, et al. Immortalization eliminates a roadblock during cellular reprogramming into iPS cells. *Nature* 2009; 460(7259): 1145–1148.

31. Hoshida Y, Villanueva A, Kobayashi M, et al. MicroRNA expression, survival, and response to interferon in liver cancer. *N Engl J Med* 2009; 361(15): 1437–1447.

32. Mima K, Okabe H, Ishimoto T, et al. CD44s regulates the TGF-β-mediated mesenchymal phenotype and is associated with poor prognosis in patients with hepatocellular carcinoma. *Cancer Res* 2012; 72(13): 3414–3423.

33. Visvader JE. Cells of origin in cancer. *Nature* 2011; 469(7330): 314–322.

34. Sell S and Leffert HL. Liver cancer stem cells. *J Clin Oncol* 2008; 26(17): 2800–2805.

35. Wagers AJ. The stem cell niche in regenerative medicine. *Cell Stem Cell* 2012; 10(4): 362–369.

36. Gish RG, Porta C, Lazar L, et al. Phase III randomized controlled trial comparing the survival of patients with unresectable hepatocellular carcinoma treated with nolatrexed or doxorubicin. *J Clin Oncol* 2007; 25(21): 3069–3075.

37. Valle J, Wasan H, Palmer DH, et al. Cisplatin plus gemcitabine versus gemcitabine for biliary tract cancer. *N Engl J Med* 2010; 362: 1273–1281.

38. National Institute for Clinical Excellence. *TA189. Sorafenib for the Treatment of Advanced Hepatocellular Carcinoma.* Londan: NICE, 2010.

39. Khan KN, Yatsuhashi H, Yamasaki K, et al. Prospective analysis of risk factors for early intrahepatic recurrence of hepatocelluar carcinoma following ethanol injection. *J Hepatol* 2000; 32: 269–278.

40. Salem R, Lewandowski RJ, Mulcahy MF, et al. Radioembolisation for hepatocellular carcinoma using Yttrium-90 microspheres: a comprehensive report of long-term outcomes. *Gastroenterology* 2010; 138: 52–64.

41. Wang SH, Lee AC, Chen IJ, et al. Structure-based optimization of GRP78-binding peptides that enhances efficacy in cancer imaging and therapy. *Biomaterials* 2016; 94: 31–44.

42. Keane MG and Pereira SP. Improving the detection and treatment of liver cancer. *Practitioner* 2013; 257(1763): 21–26.

43. Lee TY, Han-Chung Wu, Tseng YL, et al. A novel peptide specifically binding to nasopharyngeal carcinoma for targeted drug delivery. *Cancer Res* 2004; 64: 8002–8008.

44. Albert L, Lin CT, and Wu HC. Hepatocellular carcinoma cell-specific peptide ligand for targeted drug delivery. *Mol Cancer Ther* 2008; 7: 579–589.

45. Tong-Young L, Lin CT, Kuo SY, et al. Peptide-mediated targeting to tumor blood vessels of lung cancer for drug delivery. *Cancer Res* 2007; 67(22): 10958–10965.